Thai Journal of **Math**ematics
Volume 21 Number 3 (2023)
Pages 491–511

http://thaijmath.in.cmu.ac.th

ISSN 1686-0209

Stability and Optimal Control of Human T-Cell Lymphotropic Virus Type I (HTLV-I) Infection of CD4+ T-Cells which Leads to Leukemia Model with Prevention and Treatment

Ratchada Viriyapong* **and Suttipong Wuttigan**

Department of Mathematics, Faculty of Science, Naresuan University, Phitsanulok 65000, Thailand
e-mail : ratchadapa@nu.ac.th (R. Viriyapong); suttipongw61@nu.ac.th (S. Wuttigan)

Abstract Human T-lymphotropic virus type I (HTLV-I) is a retrovirus infecting CD4+ T-cells in human body with no specific treatment or vaccine. It has been linked to the adult T cell leukemia/lymphoma (ATL). A better understanding of virus dynamics is therefore essential. In this study, we propose a mathematical model describing both HTLV-I infection and leukemia of CD4+ T-cells incorporating the HTLV-I-specific CD8+ T-cells cytotoxic T-lymphocyte (CTL) response. We exhibit two biologically feasible equilibria which are infection-free and chronic infection equilibrium points. The basic reproduction number is calculated and used as a threshold clarifying equilibria stability. Optimal control problem is also investigated in this model by adding two controls namely preventive control and treatment effort control for leukemia cells. Our numerical results demonstrate that preventive control has shown to play an essential role in reducing the HTLV-I infection of CD4+ T-cells, and the treatment control can reduce leukemia cells significantly. However, a combination of both controls gives the best result in reducing HTLV-I infection and leukemia.

MSC: 34D20; 34D23; 37N25; 92B05; 49J15
Keywords: HTLV-I infection; leukemia; CD4+ T-cells; optimal control

Submission date: 08.04.2022 / Acceptance date: 12.05.2023

1. Introduction

Human T-lymphotropic virus type I (HTLV-I) is an exogeneous retrovirus that attacks the CD4+ T-cells in human body and can lead to two main types of diseases which are adult T cell leukemia/lymphoma (ATL) and HTLV-I associated myelopathy/tropical spastic paraparesis (HAM/TSP) [1, 2] HTLV-I is primarily transmitted via cell-to-cell in human through bodily fluid including sexual contact, breastfeeding, needle sharing [3]. However, there is still no clear understanding about the development of HTLV-I related diseases, no vaccine, and no satisfactory treatment.

*Corresponding author.

Published by The Mathematical Association of Thailand.

Worldwide, approximately 5-10 million people are infected with HTLV-I currently [4]. Most of HTLV-I infected people are living asymptomatic, whereas about 2-5% of HTLV-I carriers develop to ATL and about 0.25-3% develop to HAM/TSP [1, 4, 5]. However, at a present time physicians have no way of predicting which infected patients will develop ATL, where the treatment required for ATL depends on what type of ATL patients have and how it affects individually.

A mathematical model has been shown to be a good tool to further our understanding on infectious diseases either in population level or within-host level. Here in this study, we emphasize on within-host model in particular for HTLV-I infection. To the authors knowledge, Stilianakis and Seydel [6] were the first two researchers who developed an HTLV-I infection model describing the dynamics of T-cells. They divided the cells into four compartments consisting of uninfected CD4+ T-cells, latently infected CD4+ T-cells, actively infected CD4+ T-cells and leukemia cells. A few years later, Wang and colleagues [7] analyzed Stilianakis and Seydel model further in more details. In 2004, Katri and Ruan [8] modified the work of Stilianakis and Seydel further by considering a delay as a waiting period between the time when virus contacts the cell and the time when the viral RNA is incorporated into the DNA of the host genome. A year later, Gmez-Acevedo and Li [9] proposed a two-compartment model i.e., uninfected and infected T-cells which incorporates both horizontal and vertical (through mitotic proliferation) transmission. In 2006, Song and Li [10] modified Stilianakis and Seydels model by introducing the bilinear incidence term into the model. Five years later, Cai and colleagues [11] modified Song and Lis model by changing incidence term to general function. In the same year, Li and Lim [12] extended the model of Gmez-Acevedo and Li [9] by taking into account of latent period, thus it was added up to three-compartment model consisting of uninfected cells, latently infected cells and actively infected cells. In 2014, Li and Zhou [13] proposed three-compartment model consisting of healthy CD4+ T-cells, resting infected CD4+ T-cells and Tax-expressing infected CD4+ T-cells which incorporates with mitotic routes. In the same year, Lim and Maini [14] extended the model of Li and Lim [12] by incorporating viral latency and the HTLV-I-specific CTL response. Their model consisted of four compartments which were healthy CD4+ T-cells, latently infected CD4+ T-cells, actively infected CD4+ T-cells and HTLV-I-specific CD8+ or CTLs. They also represented the infected CD4+ T-cells proliferation as exponential growth term. Recently, Khajanchi and colleague [15] modified the model of Lim and Maini [14] by considering the term of elimination of actively infected CD4+ T-cells by HTLV-I specific CD8+ T-cells as bilinear incidence term. Furthermore, there are some studies of HTLV-I infection which researchers added time delay in the CTL immune response e.g., the work by Li and Shu, 2012 [16] and Song and Xu, 2021 [17]. Also, recently a few studies involving co-infection of HTLV-I and HIV has been explored e.g., the work by Elaiw and AIShamrani, 2021a [18], Elaiw and AIShamrani, 2021b [19], Elaiw and AIShamrani, 2021c [20] and AIShamrani, 2021 [21].

Motivated by above works, we propose an HTLV-I infection model to study the T-cells dynamics including ATL progression. We modify the work of Stilianakis and Seydel, 1999 [6] and Khajanchi et al., 2021 [15] by incorporating three types of cells which are CD4+ T-cells, HTLV-I-specific CD8+ T-cells or CTLs and ATL cells. The paper is started by describing how model is formulated in section 2, followed by all model analysis in section 3. Optimal control problem is also studied to seek the best strategy in reducing the HTLV-I infection and it is demonstrated in section 4. Section 5 presents the numerical solutions

in different scenarios of control conditions with discussion and finally the conclusion is in section 6.

2. Model Formulation

We propose a mathematical model describing the dynamics of CD4+ T-cells in the HTLV-I infection process. In this model, we consider the importance of the possible progression of infected CD4+ T-cells to become ATL cells and the essential role of HTLV-I-specific CD8+ T-cells or CTLs. Therefore, we further modify the work of Stilianakis and Seydel, 1999 [6] and Khajanchi et al., 2021 [15] by combining three types of cells which are CD4+ T-cells, ATL cells and HTLV-I-specific CD8+ T-cells or CTLs. Therefore, the model is divided into five compartments which are the concentration of uninfected CD4+ T-cells (X), the concentration of latently infected CD4+ T-cells (E), the concentration of actively infected CD4+ T-cells (Y), the concentration of leukemia cells (ATL cells) (L) and the concentration of HTLV-I-specific CD8+ T-cells or CTLs (H). The model schematic diagram is shown in Figure 1 and is presented as the following system of nonlinear differential equations:

$$\begin{aligned}
\frac{dX}{dt} &= \Lambda - \beta XY - \mu X,\\
\frac{dE}{dt} &= \beta XY + qY - \alpha E - \mu E,\\
\frac{dY}{dt} &= \alpha E - \theta Y - \varepsilon YH - dY - \mu Y,\\
\frac{dL}{dt} &= \theta Y + \gamma L(1 - \frac{L}{k}) - mL - \mu L,\\
\frac{dH}{dt} &= sYH - nH,
\end{aligned} \tag{2.1}$$

with initial condition

$$X(0) > 0, E(0) > 0, Y(0) > 0, L(0) > 0, H(0) > 0.$$

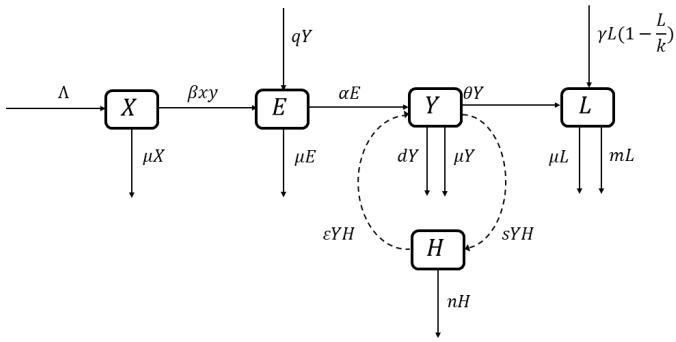

Figure 1. A schematic diagram for the HTLV-1 infection model.

The newly CD4+ T-cells are regulated at a rate λ and are assumed to be susceptible. HTLV-I infection of these cells occur when they contact the actively infected CD4+ T-cells giving a bilinear incidence term as βXY, where β is the transmission rate. These cells therefore become latently infected CD4+ T-cells. The role of mitotic division of infected cells is also considered within the model. As same as Lim and Maini, 2014 [14], we suppose that the latently infected CD4+ T-cells proliferate with an exponential rate of q representing by the term qY. The transition of latently infected CD4+ T-cells to actively infected CD4+ T-cells is represented by the term αE. The actively infected CD4+ T-cells can be eliminated by an infection at a rate d and by HTLV-I-specific CD8+ T-cells or CTLs at a rate ε, whereas they have some progression and are transferred to become leukemia cells (ATL cells) at a rate θ. Further, the leukemia cells (ATL cells) proliferate logistically at a rate γ, giving a term $\gamma L(1-\frac{L}{K})$, where K is the maximal value of leukemia cells (ATL cells). Here CD4+ T-cells die naturally at a rate μ, where the leukemia cells (ATL cells) die due to the leukemia with a rate m. The HTLV-I-specific CD8+ T-cells or CTLs are proliferated by an induced of actively infected CD4+ T-cells at a rate and decay naturally at a rate n. In this model, all parameters are positive and $\varepsilon > s$ as the CTL proliferation is a slow process [15, 16].

3. Model Analysis

3.1. Nonnegativity and Boundary of Solutions

Theorem 3.1. *For any nonnegative initial conditions, the solutions* $(X(t),E(t),Y(t),L(t),H(t))$ *of system of equations* (2.1) *are nonnegative for all* $t > 0$.

Proof. For any nonnegative initial conditions, consider the following,

$$\begin{aligned}
\frac{dX}{dt}\Big|_{X=0} &= \Lambda \geq 0,\\
\frac{dE}{dt}\Big|_{E=0} &= \beta XY + qY \geq 0,\\
\frac{dY}{dt}\Big|_{Y=0} &= \alpha E \geq 0,\\
\frac{dL}{dt}\Big|_{L=0} &= \theta Y \geq 0,\\
\frac{dH}{dt}\Big|_{H=0} &= 0.
\end{aligned}$$

Thus, all solutions of system (2.1) are nonnegative.
This completes the proof. ∎

Theorem 3.2. *All the solutions of the system* (2.1) *with nonnegative initial conditions are bounded for all* $t > 0$ *in the region* Ω *for* $\sigma > q$ *and* $\mu + m > r$.

Proof. First, let $N = X + E + Y + H$, then

$$\begin{aligned}\frac{dN}{dt} &= \frac{dX}{dt} + \frac{dE}{dt} + \frac{dY}{dt} + \frac{dH}{dt} \\ &= \Lambda - \beta XY - \mu X + \beta XY + qY - \alpha E - \mu E + \alpha E \\ &\quad -\theta Y - \varepsilon YH - dY - \mu Y + sYH - nH \\ &= \Lambda - \mu X - \mu E - \mu Y - nH + qY - dY - \theta Y - (\varepsilon - s)YH, \ \because \varepsilon > s \\ &\leq \Lambda - \min(\mu, n)N + qY. \end{aligned} \tag{3.1}$$

Since, $Y < N$, we have

$$\begin{aligned}\frac{dN}{dt} &\leq \Lambda - \min(\mu, n)N + qN \\ &= \Lambda - (\sigma - q)N, \end{aligned} \tag{3.2}$$

where, $\sigma = \min(\mu, n)$.
with integrating factor method, we have;

$$\frac{dN}{dt} + (\sigma - q)N \leq \Lambda, \tag{3.3}$$

$$e^{\int(\sigma-q)dt}\Big(\frac{dN}{dt} + (\sigma - q)N\Big) \leq \Lambda e^{\int(\sigma-q)dt}, \tag{3.4}$$

$$e^{(\sigma-q)t}\Big(\frac{dN}{dt} + (\sigma - q)N\Big) \leq \Lambda e^{(\sigma-q)t}. \tag{3.5}$$

$$N \leq \frac{\Lambda}{\sigma - q} + C_1 e^{-(\sigma-q)t}. \tag{3.6}$$

Then $N \to \dfrac{\Lambda}{\sigma - q}$ when $t \to \infty$ implying that $0 \leq N \leq \dfrac{\Lambda}{\sigma - q}$, where $\sigma > q$.
Next, consider the concentration of leukemia cells, we have

$$\begin{aligned}\frac{dL}{dt} &= \theta Y + \gamma L(1 - \frac{L}{k}) - mL - \mu L \\ &\leq \theta Y + \gamma L - mL - \mu L. \end{aligned} \tag{3.7}$$

Since, $Y \leq N \leq \dfrac{\Lambda}{\sigma - q}$, then

$$\frac{dL}{dt} \leq \theta \frac{\Lambda}{(\sigma - q)} - (\mu + m - \gamma)L. \tag{3.8}$$

Let $W = \dfrac{\Lambda}{(\sigma - q)}$, for the ease of calculation and by integrating factor, we have

$$e^{\int(\mu+m-\gamma)dt}\Big(\frac{dL}{dt} + (\mu + m - \gamma)L\Big) \leq \theta W \ e^{\int(\mu+m-\gamma)dt},$$

$$L \leq \frac{\theta W}{(\mu + m - \gamma)} + C_2 \ e^{-(\mu+m-\gamma)t}. \tag{3.9}$$

Then $L \to \dfrac{\theta W}{\mu+m-\gamma}$ when $t \to \infty$ implying that $0 \leq L \leq \dfrac{\theta W}{\mu+m-\gamma}$, where $W = \dfrac{\Lambda}{(\sigma-q)}$. Thus, the considered region for this model is

$$\Omega = \left\{(X,E,Y,L,H) \in \mathbb{R}^5_+ : N \leq \frac{\Lambda}{\sigma-q} \text{ and } L \leq \frac{\theta w}{\mu+m-\gamma}\right\}, \text{where } N = X+E+Y+H.$$

All solutions of this model are bounded and enter the region Ω for $\sigma > q$ and $\mu+m > \gamma$. Hence, Ω is a positively invariant. That is every solution of this model remains positive and bounded for all $t > 0$. ∎

3.2. Equilibrium Points

Two equilibrium points are determined as follows:
(i) Infection-free equilibrium point which is

$$E_0 = (X_0, E_0, Y_0, L_0, H_0) = \left(\frac{\Lambda}{\mu}, 0, 0, 0, 0\right).$$

(ii) The chronic infection equilibrium point is $E_1 = (X^*, E^*, Y^*, L^*, H^*)$, where

$$\begin{aligned}
X^* &= \frac{\Lambda}{\beta Y^* + \mu},\\
E^* &= \frac{\beta X^* Y^* + qY^*}{\alpha+\mu},\\
Y^* &= \frac{n}{s},\\
H^* &= \frac{1}{\varepsilon}\left[\frac{(\beta X^*+q)\alpha}{\alpha+\mu} - (\theta+d+\mu)\right], \text{and}
\end{aligned}$$

L^* is a positive solution of $A_1L^2 + A_2L + A_3 = 0$ where

$$A_1 = \frac{\gamma}{k}, A_2 = \mu+m-\gamma, A_3 = -\frac{\theta n}{s}.$$

Since $A_1 > 0$ and $A_3 < 0$, whether or not $A_2 > 0$ or $A_2 < 0$, there is one time change of sign, By Descartes's rule of sign, it guarantees that there is one positive solution L^*, and it is $L^* = \dfrac{k}{2\gamma}[\sqrt{(\mu+m-\gamma)^2 + 4\dfrac{\gamma\theta n}{ks}} - (\mu+m-\gamma)]$.

3.3. The Basic Reproduction Number (R_0)

The basic reproduction number (R_0) is the expected number of secondary cases produced by a typical infective individual. The next-generation matrix method by van den Driessche et al. [22] is used to find R_0 and we obtain

$$\mathcal{F} = \begin{bmatrix} \beta XY + qY \\ \\ 0 \end{bmatrix} \text{ and } \quad \mathcal{V} = \begin{bmatrix} \alpha E + \mu E \\ \\ \theta Y + \varepsilon YH + dY + \mu Y - \alpha E \end{bmatrix}.$$

Then,

$$F = \begin{bmatrix} 0 & \beta X + q \\ 0 & 0 \end{bmatrix} \text{ and } \quad V = \begin{bmatrix} \alpha + \mu & 0 \\ -\alpha & \theta + \varepsilon H + d + \mu \end{bmatrix}.$$

By substituting $E_0 = \left(\frac{\Lambda}{\mu}, 0, 0, 0, 0, \right)$ in F and V matrix above, we have

$$F(E_0) = \begin{bmatrix} 0 & \beta\frac{\Lambda}{\mu} + q \\ 0 & 0 \end{bmatrix} \text{ and } \quad V(E_0) = \begin{bmatrix} \alpha + \mu & 0 \\ -\alpha & \theta + d + \mu \end{bmatrix}.$$

Then,

$$V^{-1} = \frac{1}{(\alpha + \mu)(\theta + d + \mu)} \begin{bmatrix} \theta + d + \mu & 0 \\ \alpha & \alpha + \mu \end{bmatrix}.$$

The next generation matrix is

$$FV^{-1} = \begin{bmatrix} \frac{\alpha\beta\Lambda + \alpha q\mu}{\mu(\alpha + \mu)(\theta + d + \mu)} & \frac{\beta\Lambda + q\mu}{\mu(\theta + d + \mu)} \\ 0 & 0 \end{bmatrix}.$$

The basic reproduction number is given by $\rho(FV^{-1})$, which is

$$R_0 = \frac{\alpha\beta\Lambda + \alpha q\mu}{\mu(\alpha + \mu)(\theta + d + \mu)}.$$

3.4. Local Stability of Infection-Free Equilibrium Point

The Jacobian matrix of the system (2.1) is the matrix of all first-order partial derivatives of all equations with respect to X, E, Y, L and H, respectively. Hence, we have

$$J(X, E, Y, L, H) = \begin{bmatrix} -\beta Y - \mu & 0 & -\beta X & 0 & 0 \\ \beta Y & -\alpha - \mu & \beta X + q & 0 & 0 \\ 0 & \alpha & -\theta - \varepsilon H - d - \mu & 0 & -\varepsilon Y \\ 0 & 0 & \theta & \gamma(1 - \frac{2L}{k}) - \mu - m & 0 \\ 0 & 0 & sH & 0 & sY - n \end{bmatrix}. \tag{3.10}$$

Theorem 3.3. *If $R_0 < 1$, then the infection-free equilibrium point (E_0) is locally asymptotically stable. Otherwise, the infection-free equilibrium point (E_0) is unstable.*

Proof. The Jacobian matrix of the infection-free equilibrium point (E_0) is

$$J\left(X_0, E_0, Y_0, L_0, H_0\right) = \begin{bmatrix} -\mu & 0 & -\beta\frac{\Lambda}{\mu} & 0 & 0 \\ 0 & -\alpha-\mu & \beta\frac{\Lambda}{\mu}+q & 0 & 0 \\ 0 & \alpha & -\theta-d-\mu & 0 & 0 \\ 0 & 0 & \theta & \gamma-\mu-m & 0 \\ 0 & 0 & 0 & 0 & -n \end{bmatrix}. \tag{3.11}$$

From Jacobian matrix above, we set $det(J(E_0) - \lambda I) = 0$ to find eigenvalues. Thus, $\lambda_1 = -\mu < 0$, $\lambda_2 = -n < 0$, $\lambda_3 = \gamma - \mu - m < 0$, and we consider the rest of equation in the form of $\lambda^2 + a_1\lambda + a_2 = 0$, where $a_1 = \theta + d + \alpha + 2\mu > 0$, and $a_2 = \big[(\alpha+\mu)(\theta+d+\mu)\big]\big(1-R_0\big)$, when $R_0 < 1$, we obtain that $a_2 > 0$. Thus, by the Routh-Hurwitz Criterion, the infection-free equilibrium point is locally asymptotically stable, if $R_0 < 1$. When $R_0 > 1$, it is unstable. ∎

3.5. The Global Stability of the Infection-Free Equilibrium Point

Theorem 3.4. *The infection-free equilibrium point E_0 is globally asymptotically stable in Ω if $R_0 < 1$.*

Proof. In this proof, we use the method of Lyapunov functions.
Let

$$V = \alpha E + \Big(\alpha+\mu\Big)Y. \tag{3.12}$$

It is clear that V is positive definite. Then, the derivative of V along the solutions of the system (2.1) is

$$\begin{aligned} V^{'} &= \frac{\partial V}{\partial E}\cdot\frac{dE}{dt} + \frac{\partial V}{\partial Y}\cdot\frac{dY}{dt} \\ &= \alpha\Big(\beta XY + qY - \alpha E - \mu E\Big) + (\alpha+\mu)\Big(\alpha E - \theta Y - \varepsilon YH - dY - \mu Y\Big) \\ &= Y(\alpha+\mu)(\theta+d+\mu)\Big[\frac{\alpha(\beta X+q)}{(\alpha+\mu)(\theta+d+\mu)} - 1\Big] - \varepsilon YH(\alpha+\mu) \\ &\leq Y(\alpha+\mu)(\theta+d+\mu)\Big[\frac{\alpha(\beta\Lambda+q\mu)}{\mu(\alpha+\mu)(\theta+d+\mu)} - 1\Big] - \varepsilon YH(\alpha+\mu) \ \ \because X(t) \leq \frac{\Lambda}{\mu}. \end{aligned}$$

Since, $R_0 = \dfrac{\alpha(\beta\Lambda+q\mu)}{\mu(\alpha+\mu)(\theta+d+\mu)}$, then $V^{'}(t)$ above can be written as

$$V^{'} \leq Y(\alpha+\mu)(\theta+d+\mu)\Big[R_0 - 1\Big] - \varepsilon YH(\alpha+\mu).$$

We obtain that $V^{'} = 0$, when $Y = 0$ and $V^{'} < 0$ when $R_0 < 1$.
Therefore, by Lasalle's invariance principle [23] E_0 is globally asymptotically stable when $R_0 < 1$. This completes the proof. ∎

3.6. Local Stability of the Chronic Infection Equilibrium Point

Theorem 3.5. *When $R_0 > 1$, the chronic infection equilibrium point (E_1) is stable if it satisfies the Routh-Hurwitz criteria.*

Proof. Consider the Jacobian matrix of E_1 we have

$$J(E_1) = \begin{bmatrix} -\beta Y^* - \mu & 0 & -\beta X^* & 0 & 0 \\ \beta Y^* & -\alpha - \mu & \beta X^* + q & 0 & 0 \\ 0 & \alpha & -\theta - \varepsilon H^* - d - \mu & 0 & -\varepsilon Y^* \\ 0 & 0 & \theta & \gamma(1 - \frac{2L^*}{k}) - \mu - m & 0 \\ 0 & 0 & sH^* & 0 & sY^* - n \end{bmatrix}.$$

By setting $det(J(E_1) - \lambda I) = 0$, we have $\lambda_1 = \gamma(1 - \frac{2L^*}{k}) - \mu - m < 0$. The rest of equation can be considered by using the Routh-Hurwitz criteria in the form of $\lambda^4 + a_1\lambda^3 + a_2\lambda^2 + a_3\lambda + a_4 = 0$, where

$$\begin{aligned} a_1 &= \beta Y^* + \mu + \alpha + 2\mu + \theta + \varepsilon H^* + d > 0, \\ a_2 &= (\beta Y^* + \mu)(\alpha + 2\mu + \theta + \varepsilon H^* + d) + (\alpha + \mu)(\theta + \varepsilon H^* + d + \mu) \\ &\quad + (sH^*\varepsilon Y^*) - \alpha(\beta X^* + q), \\ a_3 &= (\beta Y^* + \mu)\Big[(\alpha + \mu)(\theta + \varepsilon H^* + d + \mu) + (sH^*\varepsilon Y^*) - \alpha(\beta X^* + q)\Big] \\ &\quad + (\alpha + \mu)(sH^*\varepsilon Y^*) + \beta Y^*\alpha(\beta X^*) > 0, \\ a_4 &= (\beta Y^* + \mu)(\alpha + \mu)(sH^*\varepsilon Y^*) > 0. \end{aligned}$$

Therefore, by Routh-Hurwitz criteria the chronic infection equilibrium point is stable if $a_1a_2a_3 > a_3^2 + a_1^2a_4$. ∎

3.7. Global Stability of the Chronic Infection Equilibrium Point

Theorem 3.6. *The chronic infection equilibrium point E_1 is globally asymptotically stable in Ω when $R_0 > 1$.*

Proof. We use the method of Lyapunov functions, and $W(X^*, E^*, Y^*, L^*, H^*) = 0$. At chronic infection equilibrium point, we have

$$\begin{aligned} \Lambda &= \beta X^*Y^* - \mu X^*, \\ \alpha + \mu &= \frac{\beta X^*Y^* + qY^*}{E^*}, \\ \frac{\alpha E^*}{Y^*} - \varepsilon H^* &= \theta + d + \mu, \\ n &= sY^*. \end{aligned} \tag{3.13}$$

The positive definite Lyapunov function is

$$W = (X - X^* - X^* \ln \frac{X}{X^*}) + (E - E^* - E^* \ln \frac{E}{E^*}) + (\frac{\alpha+\mu}{\alpha})(Y - Y^* - Y^* \ln \frac{Y}{Y^*}) + (\frac{\alpha+\mu}{\alpha})(\frac{\varepsilon}{s})(H - H^* - H^* \ln \frac{H}{H^*}).$$

The derivative of W along the solutions of the system (2.1) is

$$\begin{aligned} W' &= \frac{\partial W}{\partial X} \cdot \frac{dX}{dt} + \frac{\partial W}{\partial E} \cdot \frac{dE}{dt} + \frac{\partial W}{\partial Y} \cdot \frac{dY}{dt} + \frac{\partial W}{\partial H} \cdot \frac{dH}{dt}. \\ W' &= (1 - \frac{X^*}{X})(\beta X^* Y^* + \mu X^* - \beta XY - \mu X) \\ &\quad + \Big(1 - \frac{E^*}{E}\Big)(\beta XY + qY - \alpha E - \mu E) \\ &\quad + \Big(1 - \frac{Y^*}{Y}\Big)\Big(\frac{\alpha+\mu}{\alpha}\Big)(\alpha E - \theta Y - \varepsilon YH - dY - \mu Y) \\ &\quad + \Big(1 - \frac{H^*}{H}\Big)\Big(\frac{\alpha+\mu}{\alpha}\Big)\frac{\varepsilon}{s}(sYH - nH). \end{aligned}$$

Using the expressions of (3.13), we obtain

$$\begin{aligned} W' &= \mu X^*(2 - \frac{X}{X^*} - \frac{X^*}{X}) + \beta X^* Y^*(1 - \frac{X^*}{X} - \frac{XY}{X^*Y^*} - \frac{Y}{Y^*}) \\ &\quad + \beta X^* Y^*\Big(\frac{XY}{X^*Y^*} - \frac{E}{E^*} - \frac{XYE}{X^*Y^*E^*} + 1\Big) + qY^*\Big(\frac{Y}{Y^*} - \frac{E}{E^*} - \frac{YE^*}{Y^*E} + 1\Big) \\ &\quad + \beta X^* Y^*\Big(\frac{E}{E^*} - \frac{Y}{Y^*} - \frac{EY^*}{E^*Y} + 1\Big) + qY^*\Big(\frac{E}{E^*} - \frac{Y}{Y^*} - \frac{EY^*}{E^*Y} + 1\Big) \\ &\quad + \Big(\frac{\alpha+\mu}{\alpha}\Big)\Big(\varepsilon YH^* - \varepsilon YH - \varepsilon Y^*H^* + \varepsilon Y^*H\Big) \\ &\quad + \Big(\frac{\alpha+\mu}{\alpha}\Big)\Big(\varepsilon YH - \varepsilon Y^*H - \varepsilon YH^* + \varepsilon Y^*H^*\Big) \\ &= \mu X^*(2 - \frac{X}{X^*} - \frac{X^*}{X}) + \beta X^* Y^*\Big(3 - \frac{X^*}{X} - \frac{EY^*}{E^*Y} - \frac{XYE^*}{X^*Y^*E}\Big) \\ &\quad + qY^*\Big(2 - \frac{YE^*}{Y^*E} - \frac{EY^*}{E^*Y}\Big). \end{aligned}$$

By the fact that the arithmetic mean is greater than or equal to the geometric mean, we have

$$\begin{aligned} 2 - \frac{X}{X^*} - \frac{X^*}{X} &\le 0, \\ 3 - \frac{X^*}{X} - \frac{EY^*}{E^*Y} - \frac{XYE^*}{X^*Y^*E} &\le 0, \\ 2 - \frac{YE^*}{Y^*E} - \frac{EY^*}{E^*Y} &\le 0. \end{aligned}$$

This leads $W' < 0$ and $W' = 0$ when $X = X^*, E = E^*$, and $Y = Y^*$. By the LaSalle invariance principle [23] the chronic infection equilibrium point E_1 is globally asymptotically stable when $R_0 > 1$. ∎

3.8. Sensitivity Analysis of R_0

The sensitivity indices are calculated by using the technique of the normalized forward sensitivity index [24, 25] The normalized forward sensitivity index of R_0, with respect to a parameter W is given by

$$S_W^{R_0} = \frac{\partial R_0}{\partial W} \times \frac{W}{R_0}.$$

The normalized sensitivity are calculated numerically using parameter value in Table 2 and they are shown in Tabel 1.

Table 1. Numerical values of sensitivity indices of R_0

Parameter	Value	Sign
Λ	$+0.9639$	positive
β	$+0.5709$	positive
α	$+0.2500$	positive
q	$+0.0361$	positive
μ	$+0.0310$	positive
θ	-0.0006	negative
d	-0.8328	negative

4. Optimal Control Model

We next extend the system (2.1) by applying optimal control variables in the model shown in Fig. 2. For the optimal control problem, we include two control variables defined as follows:
(i) $u_1(t)$ is the preventive control e.g. safe sex.
(ii) $u_2(t)$ is the treatment effort for leukemia cells e.g. chemotherapy.

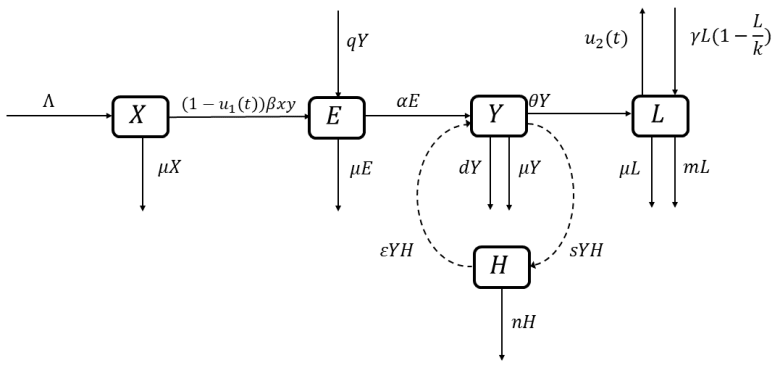

Figure 2. A schematic diagram for the optimal control problem of HTLV-I infection.

This model above can be written as system of control equations as follows:

$$\begin{aligned}
\frac{dX}{dt} &= \Lambda - (1-u_1(t))\beta XY - \mu X,\\
\frac{dE}{dt} &= (1-u_1(t))\beta XY + qY - \alpha E - \mu E,\\
\frac{dY}{dt} &= \alpha E - \theta Y - \varepsilon YH - dY - \mu Y,\\
\frac{dL}{dt} &= \theta Y + \gamma L(1-\frac{L}{k}) - mL - \mu L - u_2(t)L,\\
\frac{dH}{dt} &= sYH - nH.
\end{aligned} \tag{4.1}$$

The objective of the model is to minimize the concentration of latently infected CD4+ T-cells, actively infected CD4+ T-cells and leukemia cells at a minimal cost of control over the time interval $[0, T]$. The objective function is given by

$$J(u_1, u_2,) = \min \int_0^T \left[W_1E + W_2Y + W_3L + \frac{1}{2}\left[W_4u_1^2(t) + W_5u_2^2(t)\right] \right] dt \tag{4.2}$$

with initial conditions

$$X(0) \geq 0,\ E(0) \geq 0,\ Y(0) \geq 0,\ L(0) \geq 0, \text{ and } H(0) \geq 0.$$

Here the weight constants are denoted by W_1, W_2, W_3, W_4 and W_5 and the costs associated with preventive control and treatment effort for leukemia cell are denoted by $W_4u_1^2(t)$ and $W_5u_2^2(t)$, respectively.
The Lagrangian of the optimal control problem is given by

$$f(E, Y, L, u_1, u_2) = W_1E + W_2Y + W_3L + \frac{1}{2}\left[W_4u_1^2(t) + W_5^2(t)\right]. \tag{4.3}$$

With Pontryagins Minimum Principle (PMP), we form the Hamiltonian and derive the optimality system as follows:

$$\begin{aligned}
M &= W_1E + W_2Y + W_3L + \frac{1}{2}\left[W_4u_1^2(t) + W_5u_2^2(t)\right]\\
&\quad +\lambda_X[\Lambda - (1-u_1(t))\beta XY - \mu X] + \lambda_E[(1-u_1(t))\beta XY + qY - \alpha E - \mu E]\\
&\quad +\lambda_Y[\alpha E - \theta Y - \varepsilon YH - dY - \mu Y]\\
&\quad +\lambda_L[\theta Y + \gamma L(1-\frac{L}{k}) - mL - \mu L - u_2(t)L] + \lambda_H[sYH - nH],
\end{aligned} \tag{4.4}$$

where $\lambda_X, \lambda_E, \lambda_Y, \lambda_L$ and λ_H are the adjoint functions associated with the state equations for X, E, Y, L and H, respectively.

Theorem 4.1. *Let $\widetilde{X}, \widetilde{E}, \widetilde{Y}, \widetilde{L}$ and $\widetilde{H}$ be optimal state solution with associated optimal control variable $u_1^*(t)$ and $u_2^*(t)$ for the optimal control problem (4.1). Then there exist adjoint variables $\lambda_X, \lambda_E, \lambda_Y, \lambda_L$ and λ_H satisfying:*

$$
\begin{aligned}
\lambda_X^{'} &= -\left[\lambda_X\Big(-(1-u_1(t))\beta\widetilde{Y}-\mu\Big)+\lambda_E(1-u_1(t))\beta\widetilde{Y}\right],\\
\lambda_E^{'} &= -\left[W_1+\lambda_E(-\mu-\alpha)+\lambda_Y\alpha\right],\\
\lambda_Y^{'} &= -\Bigg[W_2+\lambda_X[-(1-u_1(t))\beta\widetilde{X}]+\lambda_E\Big[(1-u_1(t))\beta\widetilde{X}+q\Big]\\
&\quad +\lambda_Y(-\theta-\varepsilon\widetilde{H}-\mu-d)+\lambda_L\theta\Bigg],\\
\lambda_L^{'} &= -\left[W_3+\lambda_L\Big(\gamma(1-\frac{2\widetilde{L}}{k})-\mu-m-u_2(t)\Big)\right],\\
\lambda_H^{'} &= -\left[-\lambda_Y(\varepsilon\widetilde{Y})+\lambda_H(s\widetilde{Y}-n)\right],
\end{aligned}
\tag{4.5}
$$

with transversality conditions:

$$\lambda_X(T)=0,\ \lambda_E(T)=0,\ \lambda_Y(T)=0,\ \lambda_L(T)=0 \text{ and } \lambda_H(T)=0.$$

And the optimal control variables $u_1^*(t)$ *and* $u_2^*(t)$ *are*

$$
\begin{aligned}
u_1^*(t) &= max\left\{0, min\left\{\frac{(\lambda_E-\lambda_X)(\beta\widetilde{X}\widetilde{Y})}{W_4}, u_{1max}\right\}\right\},\\
u_2^*(t) &= max\left\{0, min\left\{\frac{\lambda_L\widetilde{L}}{M_5}, u_{2max}\right\}\right\}.
\end{aligned}
$$

Proof. We first differentiate Hamiltonian (4.4) with respect to X, E, Y, L and H, respectively, and the adjoint system can be calculated as

$$
\begin{aligned}
\lambda_X^{'} &= -\frac{\partial M}{\partial X} = -\left[\lambda_X\Big(-(1-u_1(t))\beta\widetilde{Y}-\mu\Big)+\lambda_E(1-u_1(t))\beta\widetilde{Y}\right],\\
\lambda_E^{'} &= -\frac{\partial M}{\partial E} = -\left[W_1+\lambda_E(-\mu-\alpha)+\lambda_Y\alpha\right]\\
\lambda_Y^{'} &= -\frac{\partial M}{\partial Y} = -\Bigg[W_2+\lambda_X[-(1-u_1(t))\beta\widetilde{X}]+\lambda_E\Big[(1-u_1(t))\beta\widetilde{X}+q\Big],\\
&\qquad +\lambda_Y(-\theta-\varepsilon\widetilde{H}-\mu-d)+\lambda_L\theta\Big]\\
\lambda_L^{'} &= -\frac{\partial M}{\partial L} = -\left[W_3+\lambda_L\Big(\gamma(1-\frac{2\widetilde{L}}{k})-\mu-m-u_2(t)\Big)\right],\\
\lambda_H^{'} &= -\frac{\partial M}{\partial H} = -\left[-\lambda_Y(\varepsilon\widetilde{Y})+\lambda_H(s\widetilde{Y}-n)\right].
\end{aligned}
\tag{4.6}
$$

Next, with the approach of Pontryagin [26], we solve the equation, $\dfrac{\partial M}{\partial u_i}=0$ at u_i^*; for $i=1,2$,

$$\frac{\partial M}{\partial u_1} = W_4 u_1(t) + \lambda_X \beta \widetilde{X}\widetilde{Y} - \lambda_E \beta \widetilde{X}\widetilde{Y} = 0,$$

$$\therefore u_1(t) = \frac{(\lambda_E - \lambda_X)\beta \widetilde{X}\widetilde{Y}}{W_4}. \tag{4.7}$$

$$\frac{\partial M}{\partial u_2} = W_5 u_2(t) - \lambda_L \widetilde{L} = 0,$$

$$\therefore u_2(t) = \frac{\lambda_L \widetilde{L}}{W_5}, \tag{4.8}$$

where $0 \leq u_1(t) \leq u_{1\max}$ and $0 \leq u_2(t) \leq u_{2\max}$.
Thus, we have

$$u_1^*(t) = \max\left\{0, \min\left\{\frac{(\lambda_E - \lambda_X)(\beta \widetilde{X}\widetilde{Y})}{W_4}, u_{1\max}\right\}\right\},$$

$$u_2^*(t) = \max\left\{0, \min\left\{\frac{\lambda_L \widetilde{L}}{M_5}, u_{2\max}\right\}\right\}. \tag{4.9}$$

This completes the proof. ∎

5. Numerical Simulation of Optimal Control

The dynamics of the system (4.1) is studied by performing numerical simulations. The forward-backward sweep method is used to solve the optimality system numerically. We consider the optimal control continuously for 450 days, with the use to the parameter values represents in Table 2. The numerical results are shown in Figure 3 - Figure 5. We divide our results into three startegies as shown below.

Table 2. Parameter values of the model used in numerical study.

Parameter	Description	Value	Unit	Ref
Λ	Influx of newly produced CD4+ T-Cells	6	day^{-1}	[6]
β	The transmission rate	0.002	-	[27]
q	The mitotic of viral transmission rate	0.045	day^{-1}	[14]
α	The rate at which latently infected CD4+ T-Cells convert spontaneously to activated cells	0.0300	day^{-1}	[28]
θ	The rate at which actively infected CD4+ T-Cells convert to ATL Cells	0.00004	day^{-1}	[6]
γ	Leukemia cell proliferation rate	0.003	day^{-1}	[6]
m	Leukemia induced death rate	0.0005	day^{-1}	Assume
d	Infection induced death rate	0.05	day^{-1}	Assume
ε	The rate of CTL-mediated lysis	0.009	-	[29]
s	The rate of CD8+T-Cells proliferation	0.007	-	[29]
k	The maximal value that ATL cells can reach	2200	cell/mm^3	[6]
μ	CD4+T-Cells natural death rate	0.01	-	[30]
n	Natural decay rate of HTLV-I-specific CD8+ T-cells or CTLs	0.4	day^{-1}	[6]

5.1. Preventive Control Alone

We use control u_1 to optimize the objective function while u_2 are set to zero. Figure 3 (a) shows that the concentration of uninfected CD4+ T-cells (X) reduces slower in the control case althought it reaches the same equilibrium value around 430 days. Figure 3 (b) shows that the concentration of latently infected CD4+ T-cells (E) increases to the peak about 70 days slower with much smaller peak in control case than non-control. Figure 3 (c) shows that in non-control case the concentration of actively infected CD4+ T-cells (Y) increases and time for the peak to occur is faster than control case about 50 days. Further, in control case there exists the second peak of (Y) 300 days after the first peak and then reduces back to same value of equilibrium as non-control case. Figure 3 (d) shows an unchange of the concentration of leukemia cells (ATL cells) (L). Figure 3 (e) shows an increase in the concentration of HTLV-I-specific CD8+ T-cells or CTLs (H) and it reaches the peak of approximately 48 in the non-control case, whereas it drops at start to zero and increases again to reach a peak on approximately 100^{th} day in control case, then comes back down to the level that lower then control case. Further, the second peak occurs 370 days after the first peak and reduces to the same equilibrium value as non-control case. Finally, Figure 3 (f) shows the strategy of u_1, that it has to be at the maximum rate of 90% for about 350 days and then decreases gradually towards zero in the 450^{th} day.

5.2. Treatment Control for Leukemia Alone

We use control u_2 to optimize the objective function while u_1 are set to zero. With this strategy, Figure 4 (a)-(c) and (e) demonstrate an unchange in the concentration of uninfected CD4+ T-cells (X), the concentration of latently of infected CD4+ T-cells (E), the concentration of actively infected CD4+ T-cells (Y) and the concentration of HTLV-I-specific CD8+ T-cells or CTLs (H) between the control and non-control one. However, Figure 4 (d) shows a dramatic decrease in the concentration of leukemia cells (ATL cells) (L) in control case comparing to non-control case which slowly decreases. From the results above, it is obtained that u_2 gives a big impact in reducing the concentration of leukemia cells (ATL cells) (L) faster. Finally, Figure 4 (f) shows the strategy of u_2, that it has to start at the maximum rate of 90% for about 7 days and and comes down to around 15% then fluctuate between 10%-25% for 20-30 days. After that it stays at approximately 12% towards the end of 450 days and reaches zero finally.

5.3. Combination of Both Controls

We use a combination of both controls to optimize the objective function. Figure 5 (a) shows that the concentration of uninfected CD4+ T-cells (X) reduces slower in the control case althought it reaches the same equilibrium value on around 420^{th} day. Figure 5 (b) shows that the concentration of latently infected CD4+ T-cells (E) increases to the peak about 70 days slower with much smaller peak in control case than non-control one. Further, the second peak occurs on 370^{th} day reaching at 300 and reduces to equilibrium value at the end. In non-control case it increases largely and reaches the peck of approximately 680. Figure 5 (c) shows that in non-control case the concentration of actively infected CD4+ T-cells (Y) increases and time for the peak to occur is faster than control case about 60 days. Further, in control case there exists the second peak of (Y) 300 days after the first peak and then reduces back to same value of equilibrium as non-control case. Figure 5 (d) shows a dramatic decrease in the concentration of leukemia

cells (ATL cells) (L) in control case comparing to non-control case which slowly decreases. Figure 5 (e) shows an increase in the concentration of HTLV-I-specific CD8+ T-cells or CTLs (H) and reaches the peak of approximately 48 in the non-control case, whereas it drops at start to zero and increases again to reach a peak on approximately 100^{th} day in control case, then comes back down to the level that lower than control case. Further, the second peak occurs 280 days after the first peak and reduces to the same equilibrium value as non-control case towards the end. Figure 5 (f) shows the strategy of u_1 that it has to be at the maximum rate of 90% for about 350 days and then decreases gradually towards zero on the 450^{th} day. Figure 5 (g) shows the strategy of u_2 that it has to start at the maximum rate of 90% for about 7 days and goes down to around 5% then fluctuates between 5%-25% for 100-120 days. After that it stays at approximately 12% and increases tiny after 380 days then it stays at 12% towards the end of 450 days and reaches zero finally. From results above, they indicate that a combination of both controls gives the best result in reducing transmission of HTLV-I and leukemia cells although the control of u_2 in this case may need to apply longer at the beginning than the case in Figure 5.

6. Conclusion

With an essential of better understanding of HTLV-I infection dynamics, we therefore propose a mathematical model describing an HTLV-I infection incorporating the possible progression of infected CD4+ T-cells to become ATL cells and the role of HTLV-I-specific CD8+ T-cells or CTLs. We modify the work of Stilianakis and Seydel, 1999 [6] and Khajanchi et al., 2021 [15] by combining three types of cells which are CD4+ T-cells, ATL cells and HTLV-I-specific CD8+ T-cells or CTLs. Therefore, our model consists of five classes which are the concentration of uninfected CD4+ T-cells (X), the concentration of latently infected CD4+ T-cells (E), the concentration of actively infected CD4+ T-cells (Y), the concentration of leukemia cells (ATL cells) (L) and the concentration of HTLV-I-specific CD8+ T-cells or CTLs (H).Within this study, mathematical analysis is performed. Positivity and boundary of solutions are proved, two equilibrium points namely infection-free and chronic infection equilibrium points are calculated and the basic reproduction number is determined. The stability of both equilibria is analyzed. We prove that if the basic reproduction number is less than unity, then no chronic HTLV-I infection would occur and the infected CD4+ T-cells will die out eventually. However, when the basic reproduction number is greater than one, then the HTLV-I infection becomes chronic with the chronic equilibrium point being global stable. Furthermore, to investigate how much prevention and/or treatment could play a role in reducing HTLV-I infection and leukemia, we extend the model above by considering the optimal control problem using Pontryagins Minimum Principle. We add two possible controls into the model and they are preventive control e.g., safe sex, and the treatment effort control for leukemia cells e.g., chemotherapy. Our numerical results of optimal control problem demonstrate a big impact of preventive control in reducing HTLV-I infection, and the treatment effort significantly reduces the leukemia cells. Furthermore, a combination of both controls gives the best result in decreasing the HTLV-I infection and leukemia. Therefore, our model could explain the dynamics more realistically as we combine all CD4+ T-cells, ATL cells and HTLV-I-specific CD8+ T-cells or CTLs classes. And the numerical results encourage the preventive control as an essential approach to reduce the infection overall.

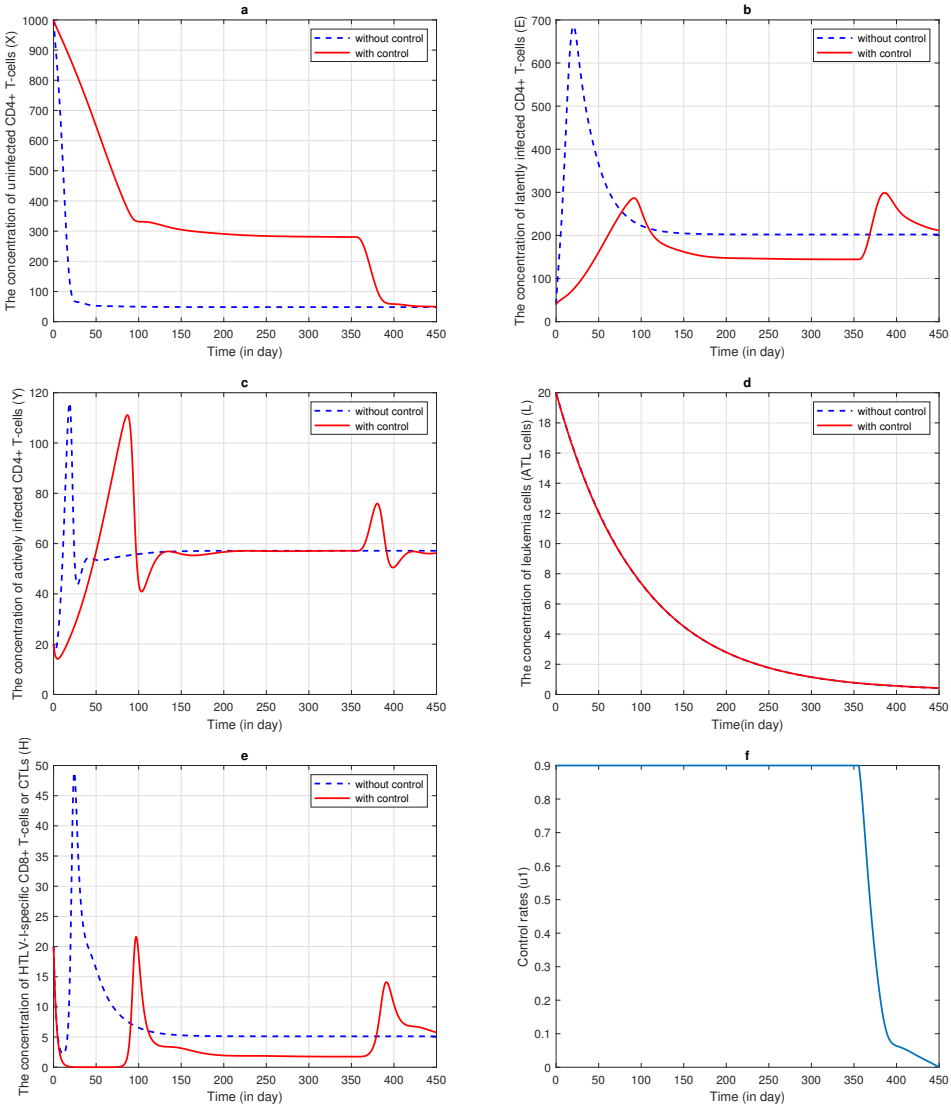

FIGURE 3. Numerical simulations of the optimal control model (4.1) with preventive control (u_1) alone. (a) the concentration of uninfected CD4+ T-cells (X), (b) the concentration of latently infected CD4+ T-cells (E), (c) the concentration of actively infected CD4+ T-cells (Y), (d) the concentration of leukemia cells (ATL cells) (L), (e) the concentration of HTLV-I-specific CD8+ T-cells or CTLs (H) and (f) the strategy of control (u_1) when u_{1max}=0.9, u_2=0.

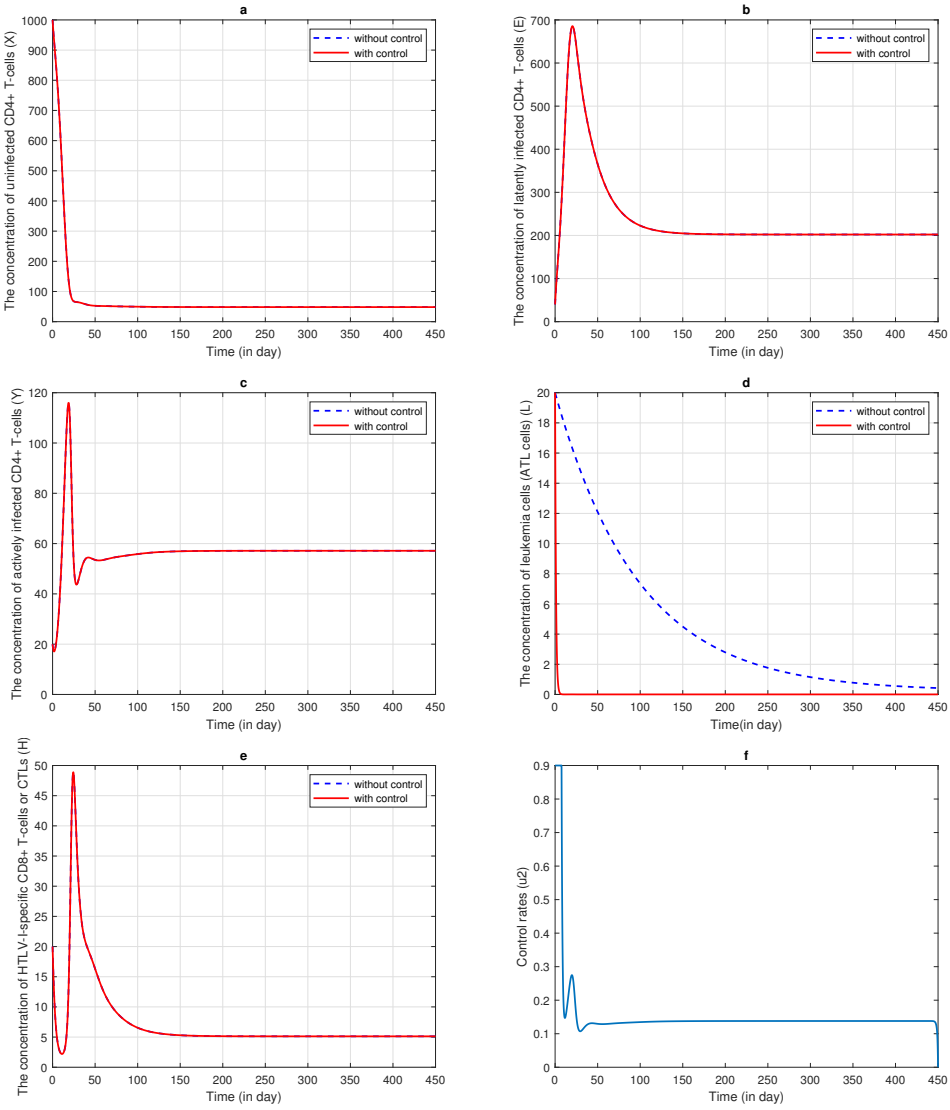

FIGURE 4. Numerical simulations of the optimal control model (4.1) with treatment control (u_2) alone. (a) the concentration of uninfected CD4+ T-cells (X), (b) the concentration of latently infected CD4+ T-cells (E), (c) the concentration of actively infected CD4+ T-cells (Y), (d) the concentration of leukemia cells (ATL cells) (L), (e) the concentration of HTLV-I-specific CD8+ T-cells or CTLs (H) and (f) the strategy of control (u_2) when u_1=0, u_{2max}=0.9.

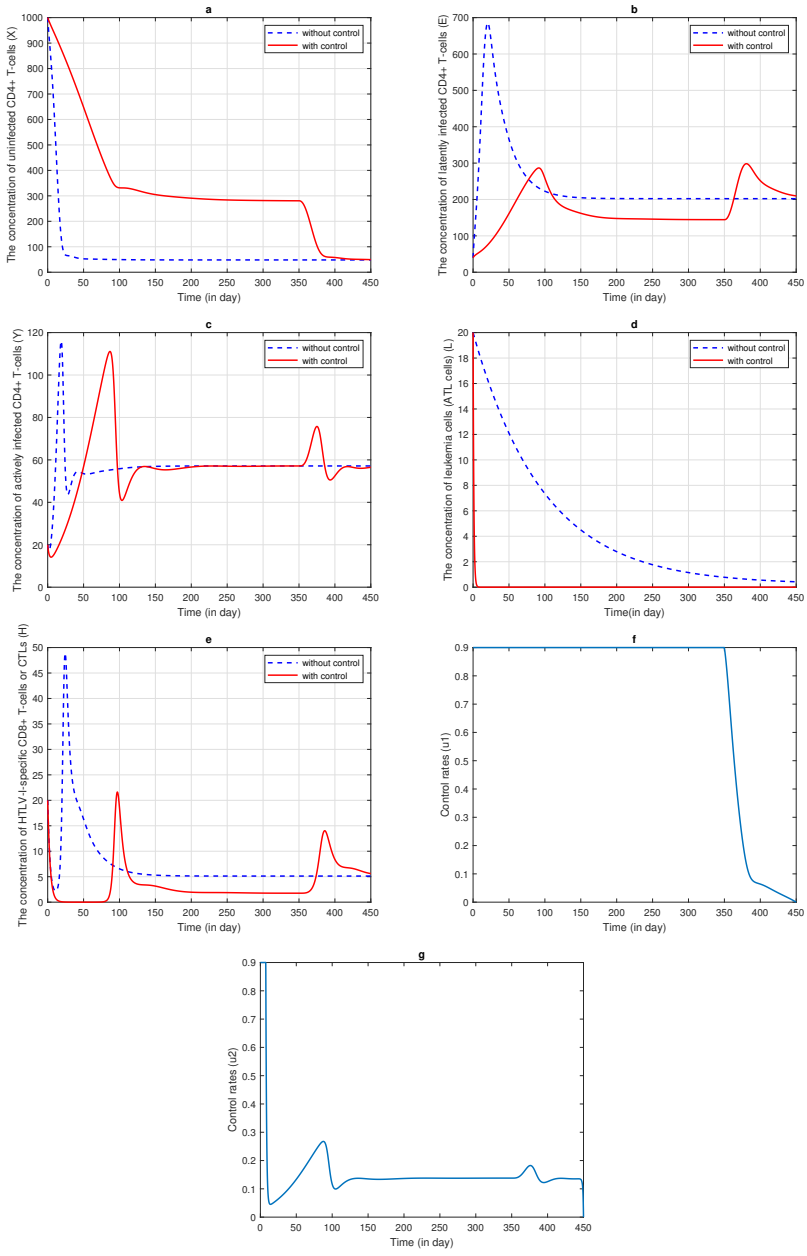

FIGURE 5. Numerical simulations of the optimal control model (4.1) with preventive control (u_1) and treatment control (u_2). (a) the concentration of uninfected CD4+ T-cells (X), (b) the concentration of latently infected CD4+ T-cells (E), (c) the concentration of actively infected CD4+ T-cells (Y), (d) the concentration of leukemia cells (ATL cells) (L), (e) the concentration of HTLV-I-specific CD8+ T-cells or CTLs (H), (f) and (g) the strategy of control (u_1) and (u_2) when u_{1max}=0.9, u_{2max}=0.9.

Acknowledgements

This work has been supported by Faculty of Science, Naresuan University, Thailand.

References

[1] F.A. Proietti, A.B.F. Carneiro-Proietti, B.C. Catalan-Soares, Global epidemiology of HTLV-I infection and associated diseases, Oncogene 24 (39) (2005) 6058–6068.

[2] R.C. Gallo, History of the discoveries of the first human retroviruses: HTLV-1 and HTLV-2, Oncogene. 24 (39) (2005) 5926–5930.

[3] M.D. Lairmore, R. Haines, R. Anupam, Mechanisms of human T-lymphotropic virus type 1 transmission and disease, Current Opinion in Virology 2 (4) (2012) 474–481.

[4] World Health Organization, Human T-lymphotropic virus type 1 (Accessed: 2022–02–05) https://www.who.int/news-room/fact-sheets/detail/human-t-lymphotropic-virus-type-1(2021).

[5] S. Tokudome, O. Tokunaga, Y. Shimamoto, Y. Miyamoto, I. Sumida, M. Kikuchi, M. Takeshita, T. Ikeda, K. Fujiwara, M. Yoshihara, T. Yanagawa, M. Nishizumi, Incidence of Adult T-Cell Leukemia/Lymphoma among Human T-Lymphotropic Virus Type I Carriers in Saga, Japan, Cancer Res. 49 (1) (1989) 226–228.

[6] N.I. Stilianakis, J. Setdel, Modeling the T-cell dynamics and pathogenesis of HTLV-I infection, Bulletin of Mathematical Biology 61 (1999) 935–947.

[7] L. Wang, M.Y. Li, D. Kirschner, Mathematical analysis of the global dynamics of a model for HTLV-I infection and ATL progression, Mathematical Biosciences 179 (2002) 207–217.

[8] P. Katri, S. Ruan, Dynamics of human T-cell lymphotropic virus I (HTLV-I) infection of CD4+ T-cells, C.R. Biologies 327 (2004) 1009–1016.

[9] H. Gómez-Acevedo, M.Y. Li, Backward bifurcation in a model for HTLV-I infection of CD4+ T cells, Bulletin of Mathematical Biology 67 (2005) 101–114.

[10] X. Song, Y. Li, Global stability and periodic solution of a model for HTLV-I infection and ATL progression, Appl. Math. Comput. 180 (2006) 401–410.

[11] L. Cai, X. Li, M. Ghosh, Global dynamics of a mathematical model for HTLV-I infection of CD4+ T-cells, Applied Mathematical Modelling 35 (7) (2011) 9587–3595.

[12] M.Y. Li, A.G. Lim, Modelling the role of tax expression in HTLV-I persistence in vivo, Bulletin of Mathematical Biology 73 (2011) 3008–3029.

[13] S. Li, Y. Zhou, Global dynamics of an HTLV-1 model with cell-to-cell infection and mitosis, Abstract and Applied Analysis 2014 (2014) 1–12.

[14] A.G. Lim, P. Maini, HTLV-I infection: a dynamic struggle between viral persistence and host immunity, Journal of Theoretical Biology 352 (2014) 92–108.

[15] S. Khajanchi, B. Sovan, T.K. Roy, Mathematical analysis of the global dynamics of a HTLV-I infection model, considering the role of cytotoxic T-lymphocytes, Mathematics and Computers in Simulation 180 (2021) 354–378.

[16] M.Y. Li., H. Shu, Global dynamics of a mathematical model for HTLV-I infection of CD4+ T cells with delayed CTL response, Nonlinear Analysis: Real World Applications 13 (2012) 1080–1092.

[17] C. Song, R. Xu, Mathematical analysis of an HTLV-I infection model with the mitosis of CD4+ T cells and delayed CTL immune response, Nonlinear Analysis: Modelling and Control 26 (1) (2021) 1–20.

[18] A.M. Elaiw, N.H. AlShamrani, Modeling and analysis of a within-host HIV/HTLV-I co-infection, Bol Soc Mat Mex. 27 (2) (2021a) 1–51.

[19] A.M. Elaiw, N.H. AlShamrani, HTLV/HIV Dual Infection: Modeling and Analysis. Mathematics 9 (2021b) 51.

[20] A.M. Elaiw, N.H. AlShamrani, Stability of HTLV/HIV dual infection model with mitosis and latency, Mathematical Biosciences and Engineering 18 (2) (2021c) 1077–1120.

[21] N.H. AlShamrani, Stability of an HTLV-HIV coinfection model with multiple delays and CTL-mediated immunity, Advances in Difference Equations 270 (2021) 1–57.

[22] P. van den Driessche, J. Watmough, Reproductive numbers and sub-threshold endemic equilibria for compartment models of disease transmission, Math. Biosci. 180 (2002) 29–48.

[23] J.P. LaSalle, The Stability of Dynamical Systems, Regional Conference Series in Applied Mathematics, SIAM, Philadelphia, 1976.

[24] M.D. Samsuzzoha, M. Singh, D. Lucy, Uncertainty and sensitivity analysis of the basic reproduction number of a vaccinated epidemic model of influenza, Appl. Math. Model. 37 (2013) 903–915.

[25] F.N. Ngoteya, Y.N. Gyekye, Sensitivity analysis of parameters in a competition model, Appl. Comput. Math. 4 (5) (2015) 363–368.

[26] L.S.V. Pontryagin, G.R. Boltyanskii, V. Gamkrelidze, E.F. Mishchenko, The Mathematical Theory of Optimal Processes, Gordon and Breach Science, New York, 1986.

[27] M.A. Nowak, R.M. May, Virus Dynamics: Mathematical Principles of Immunology and Virology, Oxford UP, Oxford, UK, 2000.

[28] B. Asquith, Y. Zhang, A.J. Mosley, C.M. de Lara, D.L. Wallace, A. Worth, L. Kaftanzi, K. Meekings, G.E. Griffin, Y. Tanaka, D.F. Tough, In vivo T lymphocyte dynamics in humans and the impact of human T-lymphotropic virus 1 infection, Proceedings of the National Academy of Sciences of the United States of America 104 (19) (2007) 8035–8040.

[29] M.Y. Li, H. Shu, Global dynamics of a mathematical model for HTLV-I infection of CD4+ T cells with delayed CTL response, Nonlinear Anal. RWA. 13 (2012) 1080–1092.

[30] D.S. Callaway, A.S. Perelson, HIV-1 infection and low steady state viral loads, Bull. Math. Biol. 64 (1) (2002) 29–64.